CrossMark

ARTICLE

Microstructures and mechanical properties of AZ91 alloys prepared by multi-pass friction stir processing

Fang Chai, Fei Yan, Wei Wang,[a] Qichen Lu, and Xiang Fang
Hubei Key Laboratory of Advanced Technology (Wuhan University of Technology), Wuhan 430070, China; Hubei Collaborative Innovation Center for Automotive Components Technology, Wuhan 430070, China; and School of Automotive Engineering, Wuhan University of Technology, Wuhan 430070, China

(Received 14 January 2018; accepted 2 April 2018)

AZ91 magnesium plates with a thickness of 6 mm were subjected to one- and two-pass friction stir processing (FSP). Microstructures and mechanical properties of the experimental materials were investigated. The results show that FSP can significantly refine the microstructures of magnesium alloys, and two-pass FSP can prepare slightly finer grains in comparison with one-pass FSP. Some coarse β-$Mg_{17}Al_{12}$ phases existed in the first pass FSP break and dissolve into the matrix under the action of the second pass FSP. Microhardness distribution of the two-pass FSP AZ91 alloy exhibits no too much difference with that of the one-pass FSP AZ91 alloy. Due to further finer microstructures, the tensile properties of the two-pass FSP alloy are slightly higher than those of the one-pass FSP alloy. Both FSP AZ91 alloys show typical ductile fracture characteristics, while the dimples on the two-pass FSP specimen are much deeper and increase in quantity.

I. INTRODUCTION

As the lightest metallic structural material, magnesium alloys have many advantages, such as low density, high specific strength and stiffness, good shock absorption, good electron-magnetic shielding effect, and easy recycling, which have a broad application prospect in the field of aerospace, automobile, and electronics.[1–3] Nevertheless, due to the hexagonal close-packed crystal structure in most magnesium alloys, they always exhibit poor formability due to the limited number of slip systems activated at room temperature. On the other hand, magnesium alloys are prone to grain coarsening and surface oxidation at high temperature. Therefore, the viability of the increasing magnesium alloy widespread application is restricted to some extent.

Up to present, a majority of research studies have reported that grain refinement can effectively solve the poor room temperature properties of magnesium alloys.[4–6] Severe plastic deformation (SPD) techniques, such as equal channel angular processing (ECAP), accumulative rolling and bonding (ARB), and high pressure torsion (HPT), have been widely used to improve the mechanical properties of magnesium alloys via refining the microstructure. Zhao et al. reported that the ultrafine-grained Mg–Nd–Zn–Zr alloy with an average grain size of around 500 nm was fabricated by an integrated extrusion and ECAP at 623 K with one pass, and the mechanical properties of the ECAPed magnesium alloy were improved because of significant grain refinement.[7] In Schwarz's study, three cycles of the ARB process led to a remarkable decrease in grain size and increase in yield strength and compression strength in the magnesium alloy AM20.[8] Torbati-Sarraf et al. demonstrated that ZK60 magnesium alloys can be successfully processed by HPT at room temperature, and HPT for 5 turns led to an equiaxed grain with an average grain size of less than 1 μm. The HTPed ZK60 magnesium alloy gained a maximum elongation of around 535% at 473 K and the initial strain rate of 1×10^{-4} s^{-1}.[9] Visibly, all these SPD approaches can refine the microstructures and thus enhance the mechanical properties for magnesium alloys.

On the other hand, as a novel solid-state SPD processing technique, friction stir processing (FSP) was proposed and developed by Mishra et al. based on the basic principles of friction stir welding (FSW). A nonconsumable high-speed rotating tool is inserted and moved transversely along the processed material which mechanically forces the material to flow in a stirring motion, and thus high microstructural densification, homogeneity, and refinement can be achieved.[10–12] Out of all the SPD approaches mentioned above, FSP is a competitive and promising method since it is a short-routine and environment friendly technique with remarkable grain-refining capacity. The FSP process can be readily conducted as bulk processing at ambient temperature, and the range of grain refinement can be controlled by the selection of different stirring tool dimensions, rotation speeds, and

[a]Address all correspondence to this author.
e-mail: wei.wang@whut.edu.cn
DOI: 10.1557/jmr.2018.98

 © Materials Research Society 2018

https://doi.org/10.1557/jmr.2018.98 Published online by Cambridge University Press

transverse speeds.[13] In recent years, researchers pay more attention to the preparation of surface/bulk metal matrix composites and ultrafine/nanograined material and research on mechanical properties at room and high temperature among FSP. Arora et al. reported that FSP resulted in significant grain refinement for the AE42 magnesium alloy, and the average grain size was refined from 20 μm in the as-cast condition to 1.5 μm. For the FSPed alloy, the yield strength and ductility improved, and the fracture surface revealed the characteristic of ductile failure with fine dimples.[14] Liang et al. fabricated carbon nanotubes reinforced magnesium nanocomposites by combining FSP and ultrasonic assisted extrusion, and the strength of magnesium nanocomposites was remarkably enhanced due to the dislocation strengthening mechanism and stress transfer mechanism.[15] Zhang et al. fabricated fine-grained AZ91 magnesium alloys with an average grain size of about 3 μm by FSP, and the elongation gained at 573 K and 1×10^{-4} s^{-1} was 1604% which indicated excellent superplasticity.[16] Visibly, FSP can remarkably refine the microstructure and thus effectively improve the mechanical properties of the processed alloys. Nevertheless, the processing parameter range for one-pass FSP to produce defect-free sheet is relatively narrow which should be selected carefully. If the processing parameters are not properly chosen, the insufficient heat input may lead to the poor metal flowability in the processing area, easily generating defects such holes and grooves. Zhang et al. studied the microstructure and mechanical properties of FSW of 2219-T6 aluminum alloys under submerging conditions, and the results showed that void defects were formed in the stir zone (SZ) at the rotation speed above 1400 rpm.[17] Mousavizade et al. conducted laser-assisted FSP of IN738LC nickel-based superalloys, and an apparent defect was examined on the advancing side of the FSP specimen. They considered that this defect was attributed to improper flow and insufficient consolidation of the metal in the FSP region.[18] In our previous experiment of conducting FSP on the hot-rolled AZ31 magnesium alloy, voids also existed on the edge of the SZ at the rotation speed of 1100 rpm and the transverse speed of 60 mm/min, while the defect disappeared as the rotation speed increased to 1300 and 1500 rpm. It is widely accepted that fabricating a defect-free FSP plate requires a condition of the shoulder-driven material merging adequately with the pin-driven material and base material. In other words, heat plays an important role in guaranteeing the quality of FSP, which further relies on the appropriate choice of rotation speed and transverse speed of the friction stir tool. However, there is a strict standard for rotation speeds and transverse speeds available for operation in the FSW welding machine. Recently multi-pass FSP is proposed, which little restricts the selection of process parameters and can successfully repair the internal defects produced in the former pass FSP by a second or third overlapping pass. Consequently, variation of the microstructure and mechanical properties in the SZ during the subsequent passes attracts the researchers' interest. EI-Rayes et al. conducted three-pass FSP with 100% overlap on 6082-T6 aluminum alloys and demonstrated that increasing the number of passes caused increasing grain size and decreasing tensile strength in the SZ.[19] Chen et al. considered that multiple process passes FSP had little effect on the microstructure and mechanical properties of 5083 aluminum alloys.[20] Brown et al. also reported that five-pass FSP on the 7050-T7451 alloy affected slightly tensile strength and microstructures in the SZ did not change during the subsequent passes.[21] On the other hand, Baruch et al. deemed that increasing the

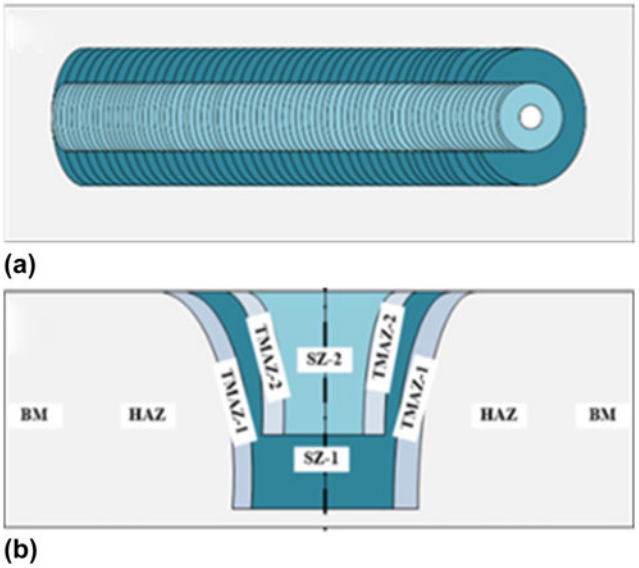


FIG. 1. Schematic representation of the multi-pass FSP in this work: (a) top surface; (b) cross section.

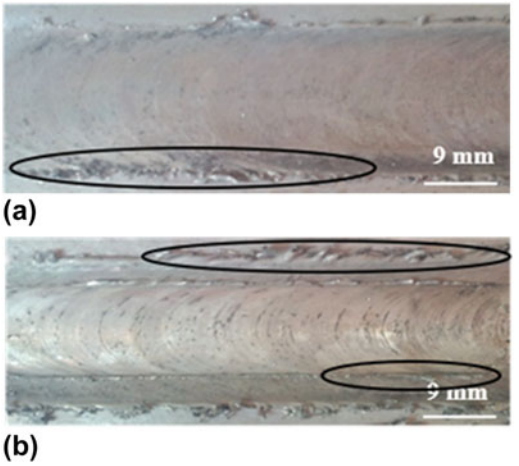


FIG. 2. Macromorphologies of the FSP specimen: (a) one-pass; (b) two-pass.

https://doi.org/10.1557/jmr.2018.98 Published online by Cambridge University Press

number of overlap passes FSP resulted in significant refinement and redistribution of the aluminum silicon eutectic phase for die cast AL–7Si–3Cu aluminum alloys.[22] Asadi et al. believed that finer grain size and enhanced hardness, strength, elongation, and wear resistance were achieved by carrying out multiple FSP of the as-cast AZ91 magnesium alloy.[23] Nakata et al. demonstrated that increasing the FSP passes could enhance the microstructural refinement.[24] Eftekhari et al. reported that increase in the FSP pass number from one to six passes resulted in the finer grain structure of the 1050 aluminum alloy.[25] It can clearly be seen that literature data about the effect of multi-pass FSP on the microstructure and mechanical properties are sometimes contradictory with respect to the different materials. Furthermore, the grain size evolution, recrystallization mechanism, and mechanical behavior due to multi-pass FSP have not been well studied. Therefore, it is necessary to carry out further research on multi-pass FSP.

In this study, an AZ91 magnesium alloy is subjected to one- and two-pass FSP, respectively. To avoid rapid growth of microstructures, a smaller friction stirring tool size which can decrease the heat input is selected for the second pass FSP. Microstructures, mechanical properties, and fracture morphologies of the experimental materials are analyzed and compared. The effect of the second pass FSP on microstructures and mechanical properties of the processed alloy is investigated.

II. EXPERIMENTAL PROCEDURE

Cast AZ91 magnesium alloy plates with a thickness of 6 mm were used in this study, and the chemical composition was 9.08Al–0.60Zn–0.27Mn–0.014Si–0.002Fe–0.012Ce (wt%). The processed plates were cleaned by acetone and fixed on the pad before processing. FSP experiments were conducted on the FSW-RT31-003 welding machine with a friction stirring tool. At the first pass FSP, the friction stir tool was composed of a shoulder with a diameter of 18 mm and a stirring pin with a bottom diameter of 4 mm and a length of 5 mm. For the second pass FSP, the friction stir tool included a shoulder with 12 mm in diameter and a stirring pin with 3 mm in length and 4 mm in diameter. The concave angle of shoulder was fixed 2.5° during processing. In this study, the AZ91 magnesium alloy was subjected to one- and two-pass FSP at a tool rotation rate of 800 rpm and a traverse speed of 60 mm/min. Figures 1(a) and 1(b) show the schematic representation of multi-pass FSP by two different sizes of the friction stirring tool on the top surface and cross section, respectively.

Microstructure examination was carried out on the cross-section perpendicular to the travel direction. After mechanically grinding and polishing, the specimens were etched by a solution of 5 g picric acid, 10 mL acetic acid, 10 mL water, and 80 mL ethanol. Microstructures of the as-cast alloy and FSP alloy at different processing zones were observed using a Leica DMI-5000M horizontal metallurgical optical microscope (OM; Leica, Solms, Germany) and a Nova Nano 430 scanning electron microscope (SEM; FEI, Eindhoven, the Netherlands). The average grain size was measured by linear-intercept method. Phase composition of the base material and the processed alloy in the SZ were analyzed by D8 advance X-ray diffraction (XRD; Bruker, Karlsruhe, Germany). The experimental condition was cooper target, and the tube voltage and current were 40 kV and 40 mA, respectively. Microhardness profiles were performed on a HVS-1000 digital hardness tester (SCTMC, Shanghai, China) with a load of 1.96 N and a dwelling time of 10 s. Tensile specimens with a gauge dimension of 3 mm in length, 2.5 mm in width, and 1.5 mm in thickness were cut by electro-discharged machining parallel to the travel direction so that the gauge parts consisted of the friction SZ only. Tensile test was conducted on a SANS-CMT-5105 machine (MTS, Shenzhen, China) at a strain rate of 1×10^{-3} s^{-1}, and the result was the average value of 5 specimens. Fracture morphologies of the tensile specimens were observed by QUATA 200 SEM (FEI, Eindhoven, the Netherlands).

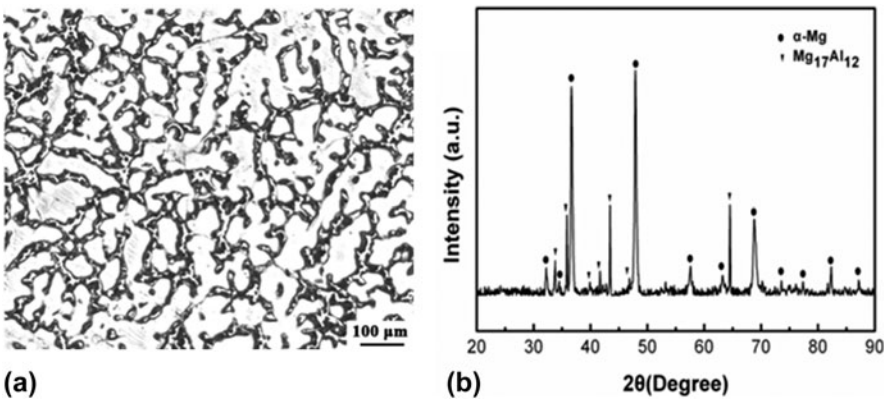


FIG. 3. As-cast AZ91 magnesium alloy: (a) OM; (b) XRD result.

https://doi.org/10.1557/jmr.2018.98 Published online by Cambridge University Press

III. RESULTS AND DISCUSSION

Figure 2 shows the macroscopic appearance of the two kinds of FSP plates on the top surface. As shown in the figure, many flashes appear both on the processing edge of the one-pass and two-pass FSP AZ91 plates. This is mainly due to the fact that the plasticized metal easily overflows along the edge of the shoulder to form flashes under double action of stirring pin and shoulder. In addition, it can be seen from Fig. 2(b) that the large size friction stirring tool produces more flashes compared with the small size friction stirring tool. With a large size friction stirring tool, increasing heat input leads to an over-plasticizing processed zone, and thus the processing surface produces more flashes.

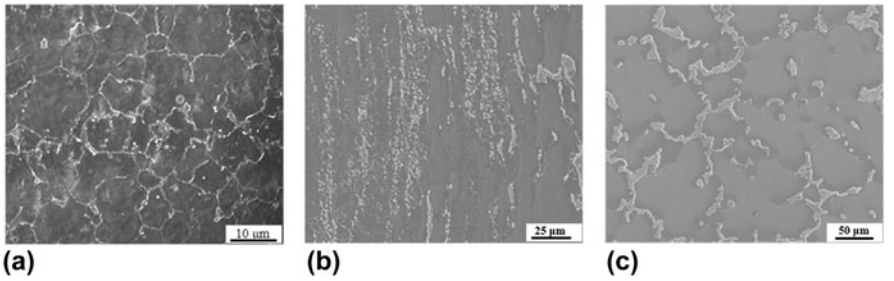


FIG. 4. SEM microstructure of the one-pass FSP AZ91 alloy: (a) SZ; (b) TMAZ; (c) HAZ.

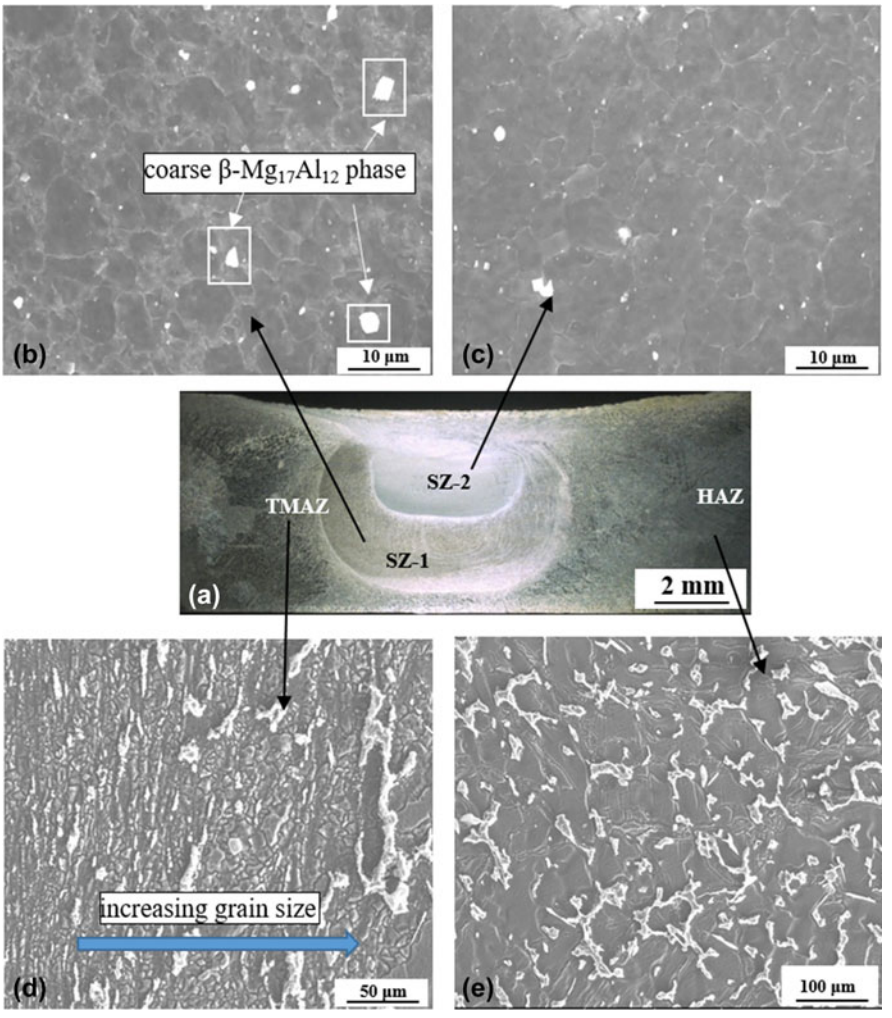


FIG. 5. Microstructures of the two-pass FSP AZ91 alloy: (a) macromorphologies on the cross-section; (b) SZ-1; (c) SZ-2; (d) TMAZ; (e) HAZ.

https://doi.org/10.1557/jmr.2018.98 Published online by Cambridge University Press

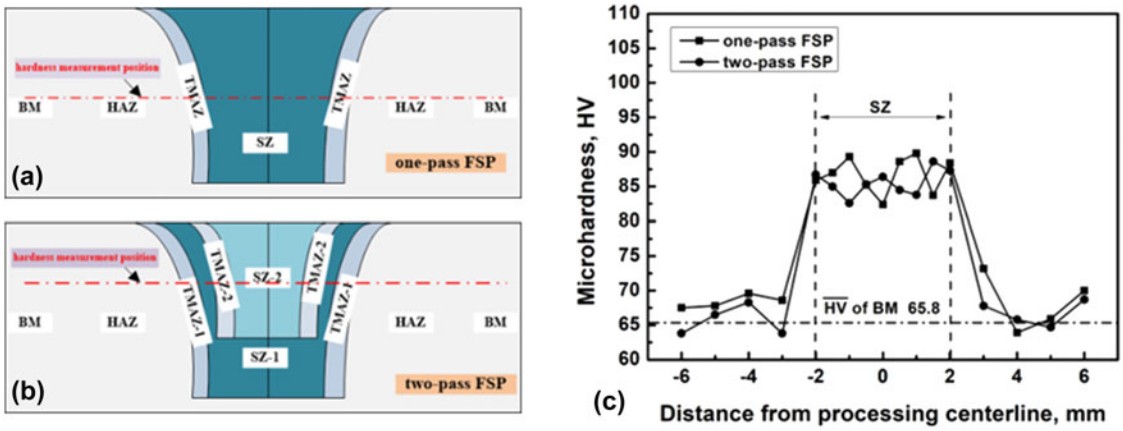


FIG. 6. (a) Hardness measurement position of the one-pass FSP alloy; (b) hardness measurement position of the two-pass FSP alloy; (c) hardness distribution on the cross-section of the as-cast, one- and two-pass AZ91 magnesium alloy.

Figure 3 shows the optical microstructure and XRD result of the AZ91 casting magnesium alloy. As shown in Fig. 3(a), AZ91 magnesium alloys are composited by two phases. Based on the result of Fig. 3(b), the two phases are α-Mg matrix and second β-$Mg_{17}Al_{12}$ phase, respectively. Combined the results of Figs. 3(a) and 3(b), the second β-$Mg_{17}Al_{12}$ phases exhibit two kinds of morphologies, i.e., most β-$Mg_{17}Al_{12}$ phases networks distribute at the grain boundaries and a few β-$Mg_{17}Al_{12}$ phases particles distribute interior the grains. The average grain size of the α-Mg alloy is about 72 μm by the mean linear-intercept method. Figure 4 shows the SEM microstructure of the one-pass FSP AZ91 magnesium alloy. Due to SPD and dynamic recrystallization, the microstructures in the SZ are significantly refined after FSP with an average grain size of approximately 7.8 μm [Fig. 4(a)]. Additionally, the coarse β-$Mg_{17}Al_{12}$ networks in the as-cast condition disappear after FSP. This is mainly due to intense friction stirring effect which leads to the second phase elongated, broken, and dissolved into the matrix. The microstructure in the thermo-mechanically affected zone (TMAZ) distributes as streamlines, and some coarse grains exist among the fine grains [Fig. 4(b)]. The grains in the heat affected zone (HAZ) exhibit a similar feature to that of the base metal [Fig. 4(c)]. Through linear-intercept method, the average grain size is about 80 μm, which is slightly larger than that of the as-cast alloy.

Figure 5 shows the macromorphology on the cross-section and microstructures of the two-pass FSP AZ91 casting alloy. As shown in Fig. 5(a), it can be seen that the processing zone is composed of three evident parts, i.e., SZ, TMAZ, and HAZ. It is worth noticing that the SZ is divided into two obvious parts, and the lower part (SZ-1) is only subjected to one-pass FSP and the upper part (SZ-2) is subjected to two-pass FSP. Figure 5(b) shows the microstructure of SZ-1. Due to the joint effect

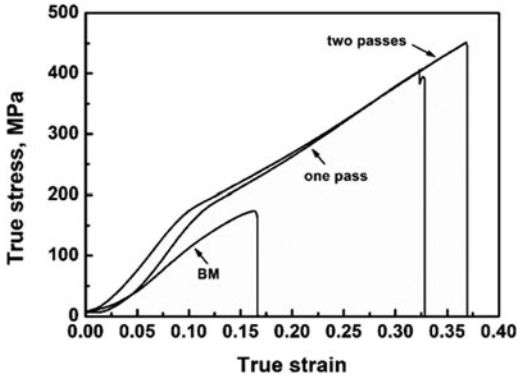


FIG. 7. True strain–true stress curve of the as-cast, one- and two-pass FSP AZ91 alloy.

of SPD and dynamic recrystallization during FSP, the average grain size in this region is about 8.1 μm. This value is slightly higher than that of the one-pass FSP AZ91 alloy, which is mainly attributed to heat input caused by the second pass FSP. Furthermore, some coarse β-$Mg_{17}Al_{12}$ phases can be examined which are marked in Fig. 5(b). Figure 5(c) shows the microstructure of SZ-2. Microstructures at this region are subjected to two times FSP, and the grains are only slightly further refined, and the average grain size is about 7.1 μm. Additionally, the number of the coarse β-$Mg_{17}Al_{12}$ phases just mentioned in Fig. 5(b) obviously decreases and fine β-$Mg_{17}Al_{12}$ particles are distributed at the grain boundaries. This is mainly due to the severe friction stirring effect in the second pass FSP which makes the coarse β-$Mg_{17}Al_{12}$ phases break and dissolve into the matrix, and reprecipitate by particles at the grain boundaries. Figure 5(d) exhibits the microstructures of TMAZ. It can be seen that the microstructures are fibrous. The coarse β-$Mg_{17}Al_{12}$ networks are significantly elongated and broken, and some small grains are distributed among

https://doi.org/10.1557/jmr.2018.98 Published online by Cambridge University Press

the elongated second phases. The microstructures near the SZ are relatively fine. With increasing distance far from the SZ, the microstructure is becoming much coarser just as the arrow demonstrates. Compared with the one-pass FSP alloy, the number of fine grains increases. Figure 5(e) shows the microstructures of the HAZ. Due to only thermal cycle effect, this area has similar microstructures to the base materials. The average grain size is about 81 μm, which is almost the same with the value of the one-pass FSP alloy in the HAZ.

Figure 6 shows the hardness measurement position and microhardness distributions on the cross section of the as-cast, one- and two-pass FSP AZ91 magnesium alloy. For the one-pass FSP specimen, the hardness measurement position is the middle line of the SZ [Fig. 6(a)]; for the two-pass FSP specimen, the hardness measurement position is the middle line of the SZ-2 [Fig. 6(b)]. The average grain size of the as-cast AZ91 magnesium alloy is about 65.8 HV. After FSP, the microhardness value in the TMAZ and HAZ shows no too much difference with that of the as-cast AZ91 alloy, while the value in the SZ increases uncommonly with an average hardness value of about 85 HV. Combined with the results of microstructure analysis, due to the effect of fine grain strengthening, solid solution strengthening, and dispersion strengthening, the SZ has the maximum microhardness value. Moreover, microhardness distribution of the one- and two-pass FSP AZ91 alloy is almost the same, indicating the second pass FSP has little effect on the microhardness distribution in this study.

Figure 7 shows the true stress–true strain curve of the as-cast, one and two-pass FSP AZ91 alloys. Table I summarizes the tensile properties of the AZ91 magnesium alloy. Due to the existence of coarse β-$Mg_{17}Al_{12}$ second phases distributed at the grain boundaries, the AZ91 casting alloy is easily cracked and debonded from the α-Mg matrix under lower stress. Therefore, the as-cast AZ91 magnesium alloy exhibits poor tensile properties with an ultimate tensile strength of 148 MPa and an elongation of 15.6%. After FSP, the microstructure of the α-Mg matrix is remarkably refined, and the second network phases are broken and dissolved into the matrix

TABLE I. Tensile properties of the as-cast, one and two-pass FSP AZ91 alloys.

Alloy	Yield strength/MPa	Ultimate tensile properties/MPa	Elongation/%
As-cast	115	148	15.6
One-pass	147	294	25.2
Two-pass	156	312	29.4

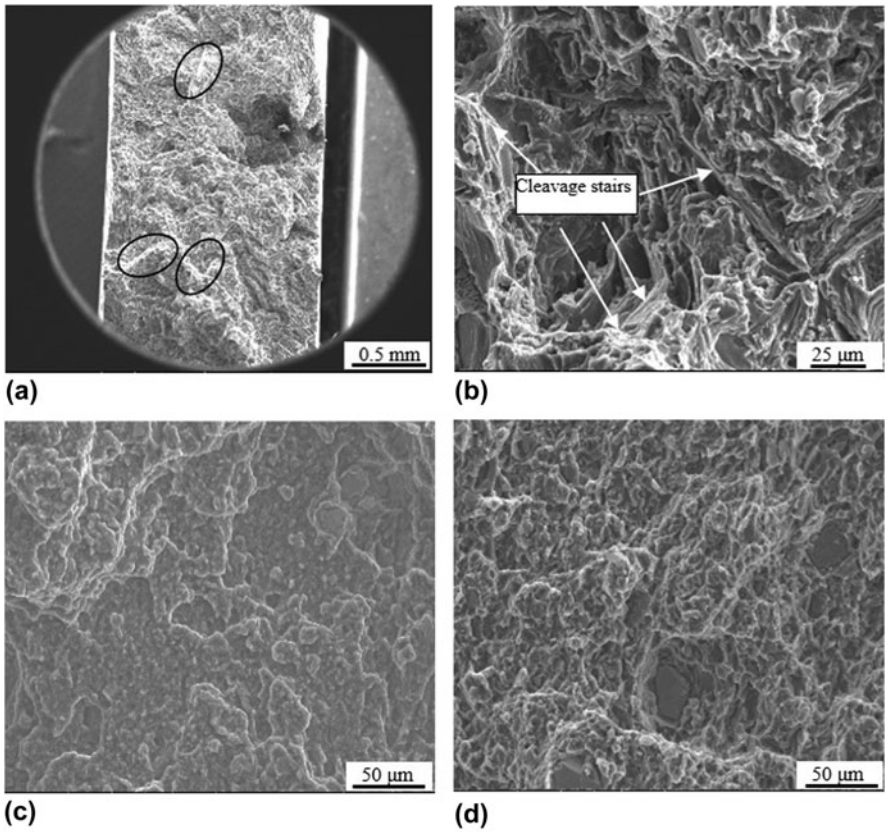


FIG. 8. Fracture surface morphologies of the as-cast and FSP AZ91 alloy: (a and b) as-cast; (c) one-pass; (d) two-pass.

https://doi.org/10.1557/jmr.2018.98 Published online by Cambridge University Press

and reprecipitate by the β-$Mg_{17}Al_{12}$ particles. Compared with the as-cast AZ91 magnesium alloy, the tensile strength significantly improves with a value of 294 MPa. Moreover, finer microstructures make the tensile deformation more uniform, and the elongation of the one-pass FSP AZ91 magnesium alloy is 25.2%, which is about 1.6 times the size of the as-cast AZ91 magnesium alloy. Both the ultimate tensile strength and elongation further slightly improve in the two-pass FSP AZ91 alloy with a value of 312 MPa and 29.4%. Evidently, FSP can significantly make better the tensile strength and elongation of the as-cast AZ91 alloy, and the second pass FSP can further briefly increase the tensile properties via refining and homogenizing the microstructures.

Figure 8 shows the fracture surface morphologies of the as-cast, one- and two-pass FSP AZ91 magnesium alloys. Figures 8(a) and 8(b) show the fracture surface morphologies of the as-cast AZ91 magnesium alloy. As shown in Fig. 8(a), the fracture surface is relatively flat. Some bright crystalline surface (as marked in the figure) and small pores can be observed, indicating typical quasi-dissociation fracture characteristics. Figure 8(b) shows the enlarged view of the fracture surface of the AZ91 casting alloy. Some cleavage stairs can be clearly observed that are marked by arrows. Figures 8(c) and 8(d) show the fracture morphologies of the one- and two-pass FSP AZ91 alloy, respectively. Dimples and tearing edges appear on the fracture surfaces of the FSP AZ91 alloy, which suggests ductile fracture. This is due to the increasing plasticity caused by FSP. Comparing Figs. 8(c) and 8(d), dimples on the fracture surface of the two-pass FSP AZ91 magnesium alloy are much deeper and more in number.

IV. CONCLUSIONS

In this study, cast AZ91 magnesium alloys are subjected to one- and two-pass FSP, respectively. Microstructures and mechanical properties of the experimental materials are investigated. The conclusions are obtained as following:

(1) FSP results in the remarkable α-Mg matrix refinement and the second β-$Mg_{17}Al_{12}$ phase breakup and dissolution. Compared with one-pass FSP, the second pass FSP can further slightly refine the microstructures of AZ91 magnesium alloys and lead to some coarse second β-$Mg_{17}Al_{12}$ phase dissolved into the matrix.

(2) Due to the effect of fine grain strengthening, solution strengthening and dispersion strengthening, the microhardness in the SZ, ultimate tensile strength, and elongation are all enhanced to some extent. The ultimate tensile strength and elongation of the two-pass FSP increase from one-pass FSP of 294 MPa and 25.2% to 312 MPa and 29.4%.

(3) The as-cast AZ91 magnesium alloy exhibits quasi-dissociation fracture, while the one and two-pass FSP AZ91 alloys present ductile fracture.

ACKNOWLEDGMENTS

This work was supported by the Fundamental Research Funds for Central University under Grant Nos. (WUT: 2017IVA033 and WUT: 2016IVA032), the 111 Project (B17034) and Open Foundation of National Engineering Research Center of Near-net-shape Forming for Metallic Materials of South China University of Technology under Grant No. 201510.

REFERENCES

1. S. Fooladi and S.R. Kiahosseini: Creation and investigation of chitin/HA double-layer coatings on AZ91 magnesium alloy by dipping method. *J. Mater. Res.* **32**, 2532 (2017).
2. B.L. Mordike and T. Ebert: Magnesium properties applications potential. *Mater. Sci. Eng., A* **302**, 37 (2001).
3. H. Shan, Y. Zhang, Y. Li, and Z. Luo: Dissimilar joining of AZ31B magnesium alloy and pure copper via thermo-compensated resistance spot welding. *J. Manuf. Process.* **30**, 570 (2017).
4. A.H. Feng and Z.Y. Ma: Enhanced mechanical properties of Mg–Al–Zn cast alloy via friction stir processing. *Scripta Mater.* **56**, 397 (2007).
5. K. Bryla, J. Morgiel, M. Faryna, K. Edalati, and Z. Horita: Effect of high-pressure torsion on grain refinement, strength enhancement and uniform ductility of EZ magnesium alloy. *Mater. Lett.* **212**, 323 (2018).
6. S. Amani, G. Faraji, and K. Abrinia: Microstructure and hardness inhomogeneity of fine-grained AM60 magnesium alloy subjected to cyclic expansion extrusion (CEE). *J. Manuf. Process.* **28**, 197 (2017).
7. S. Zhao, E. Guo, G.J. Cao, L.P. Wang, Y.C. Lun, and Y.C. Feng: Microstructure and mechanical properties of Mg–Nd–Zn–Zr alloy processed by integrated extrusion and equal channel angular pressing. *J. Alloys Compd.* **705**, 118 (2017).
8. F. Schwarz, C. Eilers, and L. Krüger: Mechanical properties of an AM20 magnesium alloy processed by accumulative roll-bonding. *Mater. Charact.* **105**, 144 (2015).
9. S.A. Torbati-Sarraf and T.G. Langdon: Properties of a ZK60 magnesium alloy processed by high-pressure torsion. *J. Alloys Compd.* **613**, 357 (2014).
10. R.S. Mishra and Z.Y. Ma: Friction stir welding and processing. *Mater. Sci. Eng., R* **50**, 1 (2005).
11. S.Y. Xie, R.D. Li, T.C. Yuan, C. Chen, K.C. Zhou, B. Song, and Y.S. Shi: Laser cladding assisted by friction stir processing for preparation of deformed crack-free Ni–Cr–Fe coating with nanostructure. *Opt. Laser Technol.* **99**, 374 (2018).
12. P. Vijayavel and V. Balasubramanian: Effect of pin profile volume ratio on microstructure and tensile properties of friction stir processed aluminum based metal matrix composites. *J. Alloys Compd.* **729**, 828 (2017).
13. A. Raja and V. Pancholi: Effect of friction stir processing on tensile and fracture behavior of AZ91 alloy. *J. Mater. Process. Technol.* **248**, 8 (2017).
14. H.S. Arora, H.S. Grewal, H. Singh, B.K. Dhindaw, and S. Mukherjee: Enhancing the mechanical properties of AE42 magnesium alloy through friction stir processing. *Adv. Eng. Mater.* **16**, 571 (2014).
15. J.H. Liang, H.J. Li, L.H. Qi, W.L. Tian, X.F. Li, X.J. Chao, and J.F. Wei: Fabrication and mechanical properties of CNTs/Mg

https://doi.org/10.1557/jmr.2018.98 Published online by Cambridge University Press

composites prepared by combining friction stir processing and ultrasonic assisted extrusion. *J. Alloys Compd.* **728**, 282 (2017).
16. D.T. Zhang, S.X. Wang, C. Qiu, and W. Zhang: Superplastic tensile behavior of a fine-grained AZ91 magnesium alloy prepared by friction stir processing. *Mater. Sci. Eng., A* **556**, 100 (2012).
17. H.J. Zhang, H.J. Liu, and L. Yu: Microstructure and mechanical properties as a function of rotation speed in underwater friction stir welded aluminum alloy joints. *Mater. Des.* **32**, 4402 (2011).
18. S.M. Mousavizade, M. Pouranvari, F.M. Ghaini, H. Fujii, and Y.D. Chung: Laser-assisted friction stir processing of IN738LC nickel-based superalloy: Stir zone characteristics. *Sci. Technol. Weld. Join.* **21**, 374 (2016).
19. M.M. El-Rayes and E.A. El-Danaf: The influence of multi-pass friction stir processing on the microstructural and mechanical properties of aluminum alloy 6082. *J. Mater. Process. Technol.* **212**, 1157 (2012).
20. Y. Chen, H. Ding, J. Li, Z. Cai, J. Zhao, and W. Yang: Influence of multi-pass friction stir processing on the microstructure and mechanical properties of Al-5083 alloy. *Mater. Sci. Eng., A* **650**, 281 (2016).
21. R. Brown, W. Tang, and A.P. Reynolds: Multi-pass friction stir welding in alloy 7050-T7451: Effects on weld response variables and on weld properties. *Mater. Sci. Eng., A* **513–514**, 115 (2009).
22. L.J. Baruch, R. Raju, V. Balasubramanian, A.G. Rao, and I. Dinaharan: Influence of multi-pass friction stir processing on microstructure and mechanical properties of die cast Al–7Si–3Cu aluminum alloy. *Acta Metall. Sin.* **29**, 431 (2016).
23. P. Asadi, G. Faraji, and M.K. Besharati: Producing of AZ91/SiC composite by friction stir processing (FSP). *Int. J. Adv. Manuf. Technol.* **51**, 247 (2010).
24. K. Nakata, Y.G. Kim, H. Fuji, T. Tsumura, and T. Komazaki: Improvement of mechanical properties of aluminum die casting alloy by multi-pass friction stir processing. *Mater. Sci. Eng., A* **437**, 274 (2006).
25. M. Eftekhari, M. Movahedi, and A.H. Kokabi: Microstructure, strength and wear behavior relationship in Al–Fe_3O_4 nanocomposite produced by multi-pass friction stir processing. *J. Mater. Eng. Perform.* **26**, 3516 (2017).

https://doi.org/10.1557/jmr.2018.98 Published online by Cambridge University Press